Cell Calcium 77 (2019) 8–19

Contents lists available at ScienceDirect

Cell Calcium

journal homepage: www.elsevier.com/locate/ceca

Downregulation of TRPC6 expression is a critical molecular event during FK506 treatment for overactive bladder

Cheng Chang[a], Kai Li[b], Sinan Jiang[a], Baoman Li[c], Liu Cao[d], Ping Wang[a,*]

[a] Department of Urology, the Fourth Affiliated Hospital of China Medical University, No.4, Chong-shan East Road, Shenyang 110032, Liaoning Province, PR China
[b] Department of Surgical Oncology, the First Affiliated Hospital of China Medical University, No.155, Nan-jing North Street, Shenyang 110001, Liaoning Province, PR China
[c] Department of Brain Metabolic Diseases Laboratory, Institute of Metabolic Disease Research and Drug Development, China Medical University, No.77, Puhe Road, Shenyang 110122, Liaoning Province, PR China
[d] Department of Key Laboratory of Medical Cell Biology (Ministry of Education), the Institute of Translational Medicine, China Medical University, No.77, Puhe Road, Shenyang 110122, Liaoning Province, PR China

ARTICLE INFO

Keywords:
OAB
FK506
TRPC6
BSMC
PDGF
Calcium

ABSTRACT

Purpose: It has been suggested that FK506 could improve some symptoms of OAB in both clinical settings and animal models; however, its mechanism of action is not well-understood. Here, we investigated the effect of FK506 on TRPC6 in bladder smooth muscle, and explored the possible involvement of TRPC6 in OAB.
Methods: FK506 was injected intraperitoneally into rats in which OAB was induced via BOO, and urodynamic indices were recorded. Rats and human bladder smooth muscle tissues with or without OAB were examined for TRPC6 expression by western blot, RT-PCR and IF staining. Cultured BSMCs were treated with PDGF, TRPC6 siRNAs and FK506. Then the TRPC6 expression and cellular proliferation were examined, and the Ca^{2+} influx and contractility of BSMCs were examined by time-lapse Ca^{2+} imaging and collagen gel contraction. Finally, IF and Co-IP were performed to test the effects of FK506 on NFAT translocation to the nucleus and the interaction of TRPC6 with FKBP12, respectively.
Results: FK506 improved urodynamic indices of OAB rats, and TRPC6 was expressed in rats and human bladder tissues. TRPC6 elevation in OAB rats was inhibited by FK506, and this inhibition coincided with improvements in urodynamic indices. PDGF enhanced TRPC6 expression, cellular proliferation, Ca^{2+} influx and contractility of BSMCs, and these effects were inhibited by TRPC6 siRNAs and FK506. FK506 inhibited NFAT translocation to the nucleus and disrupted the interaction of TRPC6 with FKBP12.
Conclusions: Our results collectively indicate that FK506 may be used to treat OAB, and that TRPC6 may serve as an attractive target for therapeutic intervention in OAB.

1. Introduction

Overactive bladder (OAB) is a common urodynamic dysfunction that is characterized by symptoms of urgency, frequency, and nocturia. The bladder outlet obstruction (BOO) is one of the main causes of OAB [1]. Urodynamic assessments typically show detrusor instability in patients with OAB [2]. Because a variety of receptors and ion channels play pivotal roles in regulating both contraction and relaxation of bladder smooth muscle tissue, treatment with antimuscarinics is the current mainstay for clinical management of OAB. Other drugs, such as immunosuppressant agent FK506 (Tacrolimus), have also been found to improve some OAB voiding symptoms of radiation cystitis (RC) or hemorrhagic cystitis (HC) (i.e., reductions inurinary frequency and increases in the inter contraction interval) in both clinical cases and animal models [3–6]. Whether these drugs act through ion channels during this process, however, remains largely unknown. Thus, this

Abbreviations: OAB, overactive bladder; BOO, bladder outlet obstruction; RC, radiation cystitis; HC, hemorrhagic cystitis; TRPC, transient receptor potential canonical; BSMC, bladder smooth muscle cell; ICI, inter contraction interval; MCC, maximum cystometric capacity; Pves, vesical pressure; Pabd, abdominal pressure; BC, bladder compliance; NVC, non-voiding contractions; Pmax, maximal detrusor pressure; PDGF, platelet derived growth factor; VEGF, vascular endothelial growth factor; PI, propidium iodide; FBS, fetal bovine serum; BSA, bovine serum albumin; DMEM, dulbecco's modified eagle media; TG, thapsigargin; RT-PCR, reverse transcription-polymerase chain reaction; qPCR, real-time quantitative PCR; IF, immunofluorescence; Co-IP, co-immunoprecipitations; IOD, integrated optical density; PC, positive control

* Corresponding author.
E-mail address: pwang@cmu.edu.cn (P. Wang).

https://doi.org/10.1016/j.ceca.2018.11.007
Received 6 May 2018; Received in revised form 11 November 2018; Accepted 16 November 2018
Available online 17 November 2018

study first aimed to examine and confirm whether FK506 could ameliorate the symptoms of OAB induced in rats via BOO.

FK506 is known to exert many of its biological functions by binding to its partner FKBP12, and FKBP12 is a necessary component of some ion channels such as the transient receptor potential canonical 6 (TRPC6), a non-selective calcium channel. It has been reported that FK506 exerts renoprotective effects by suppressing the activity and inhibiting the expression of the TRPC6 channel, possibly by disrupting the interaction between FKBP12 and TRPC6 [7–10]. The TRPC channel family comprises seven non-selective cation channels (TRPC1-7) [11]. Similarly to other TRP families, TRPCs also consist of six distinct protein families and can transport Na^+, Ca^{2+} and Mg^{2+}. Among these, TRPC6, which can transport Ca^{2+}, has been well-studied regarding its role in smooth muscle contraction. In the circulatory system, TRPC6-mediated Ca^{2+} influx is required for Ang II-induced cardiomyocyte hypertrophy [12]. In the digestive system, TRPC6 activation promotes depolarization of intestinal smooth muscle cells, thereby affecting smooth muscle contraction [13]. It has been reported that only TRPC4 and TRPC6 are expressed in isolated murine detrusor myocytes [14]. Gevaert et al. reported that the deletion of TRPV4 impaired the bladder voiding in mice, suggesting that TRPV4 is also important in regulating the function of the bladder [15]. However, until now, there have been no reports detailing a role for TRPC6 in FK506-mediated treatment of OAB. Thus, we examined and confirmed the effect of FK506 on TRPC6 expression in bladder smooth muscle of OAB rats and whether TRPC6 inhibition was consistent with an improvement in OAB symptoms.

According to prior reports, platelet derived growth factor (PDGF) is one of the most important growth factors in bladder remodeling [16,17], and stimulates pulmonary vascular smooth muscle cell proliferation by upregulating TRPC6 expression [18]. Thus we examined the effect of PDGF and FK506 on TRPC6 expression and cellular proliferation in bladder smooth muscle cells (BSMCs). SAR7334, as a specific inhibitor of TRPC6, was recently discovered and found to reduce TRPC6-mediated Ca^{2+} influx (with an IC_{50} of 9.5 nM) and TRPC6 currents (with an IC_{50} of 7.9 nM) in TRPC6-HEK-FITR cells [19–21]. Finally, we used SAR7334 and FK506 in cell-based assays to further test their effects on TRPC6 channel function and the contractility of BSMCs.

Through these analyses, we confirmed that FK506 can improve the urodynamic symptoms of OAB caused by BOO. We further provide evidence supporting a possible role for TRPC6 in bladder smooth muscle. Downregulation of TRPC6 expression may be a critical molecular event during FK506 treatment for OAB. Our findings thus provide potentially supplement for myogenic basis of OAB.

2. Materials and methods

2.1. Reagents

PDGF and vascular endothelial growth factor (VEGF) were obtained from R&D Systems (Minneapolis, MN, USA). Fetal bovine serum (FBS) was obtained from Life Technologies (Carlsbad, CA, USA). Dulbecco's modified eagle media (DMEM)/F-12 was obtained from Hyclone (Logan, UT, USA). Opti-modified eagle media (Opti-MEM™) was obtained from Gibco (Thermo Fisher Scientific, Waltham, MA, USA). FK506 was obtained from Tacrolimus (Astellas, Japan). SAR7334 was obtained from Med Chem Express (Monmouth Junction, NJ, USA). Thapsigargin (TG) was obtained from Meilun Biotechnology (Dalian, China). The type-I collagen, Hanks and D-Hanks solutions were obtained from Solarbio Biotechnology (Beijing, China). Anti-β-actin antibody and propidium iodide (PI) obtained from Dingguo-Changsheng Biotechnology (Beijing, China). Anti-α-SMA antibody was obtained from Boster Biotechnology (Wuhan, China). Donkey anti-rabbit IgG (H + L) highly cross-adsorbed secondary antibody (Alexa Fluor 488), Trizol, bovine serum albumin (BSA), Lipofectamine™ 3000 Reagent, Fluo-4/AM and F-127 were obtained from Life Invitrogen (Thermo Fisher Scientific, Waltham, MA, USA). Anti-FKBP12 monoclonal antibody of rats (554,091) was from BD Pharmingen/Transduction Laboratories (San Diego, CA). Anti-NFATc4 antibody of rats (SC-271597) was from Santa Cruz Biotechnology (Santa Cruz, CA, USA). Anti-TRPC6 antibodies of human (SAB2102583) and rats (T6442), and all other chemicals were obtained from Sigma-Aldrich (Saint Louis, MO, USA).

2.2. Animals

Adult female Wistar rats, weighting 225 ± 6.3 g, were purchased from the Experimental Center of China Medical University. Rats were housed in containment facilities at the Animal Center and maintained on a regular 12/12 h light/dark cycle with free access to food and water. All animal experimental protocols and procedures were performed in accordance with the ARRIVE guidelines, and carried out in accordance with the U.K. Animals (Scientific Procedures) Act, 1986 and associated guidelines, EU Directive 2010/63/EU for animal experiments, and the National Institutes of Health guide for the care and use of Laboratory animals (NIH Publications No. 8023, revised 1978), and also approved by the Animal Experimental Committee of China Medical University.

2.3. Clinical samples

Clinical samples were collected from patients, including four with OAB (OAB group, patients with benign prostatic hyperplasia) and four without OAB (control group, patients with bladder tumor) by urinary dynamic detection. The experiment was performed in accordance with the principles of Declaration of Helsinki, registered at The Fourth Affiliated Hospital of China Medical University and conducted between 2014 and 2015 with informed consent of patients and ethical committee approval. Also the privacy rights of human subjects were always be observed.

2.4. Cell culture

BSMCs of rats (CHI Scientific, Jiangsu, China) were cultured in DMEM/F-12 supplemented with 10% FBS at 37 °C in a humidified incubator with an atmosphere of 5% CO_2. Cells were cultured in 10 cm dishes and the medium was changed every 1–2 days. Cells were subcultured every 3–4 days, and all experiments were performed using cells from passages 2-4. For experiments, BSMCs were cultured in DMEM/F-12 containing 1% FBS with or without the indicated treatments.

2.5. Animal model

Twelve rats were randomly divided into three groups of four rats each: groups A, B and C. During the surgical procedure, the rats were injected intraperitoneally with 5% chloral hydrate for anesthesia (3 mL/kg body weight). The abdomen was opened through a low midline abdominal incision to fully expose the bladder neck and proximal urethra. To establish the OAB model, rats from groups B and C underwent bladder neck ligation. To achieve this, two PVC tubes (diameter 1.2 mm) were respectively inserted and located under (in the vagina) and above (in the abdomen) the bladder neck, then the tubes were squeezed against the urethra using a 4-0 silk ligature. The tightness of the ligature was adjusted so that the catheter could slowly and uniformly slide out when attached to a 2 g weights. As controls, rats from group A had their bladder neck and proximal urethra exposed, but didn't undergo bladder neck ligation. The abdominal wall was sutured using 3-0 silk and then antibiotics (penicillin G, 200,000 IU/kg and streptomycin, 300,000 IU/kg; i.m.) were administered.

Four weeks following the operation, rats from groups A and B were injected intraperitoneally with a solution of 5% glucose (0.1 mL/day) for 14 days, whereas rats in group C were injected intraperitoneally

with FK506 (0.1 mg/kg/day, was also diluted in 5% glucose) for 14 days [22].

2.6. Urinedynamic testing

Six weeks after the operation, urodynamic indices were measured. Following anesthesia via intraperitoneal injection of 5% chloral hydrate (3 mL/kg body weight), rats from the three groups had two indwelling fistulation catheters (external diameter 1.0 mm, internal diameter 0.6 mm) inserted percutaneously. One indwelt catheter was inserted into the bladder dome and was used to measure vesical pressure (Pves), and the other was inserted into the abdomen and was used to measure abdominal pressure (Pabd). The catheters were affixed to the skin with a 3-0 silk ligature. This percutaneous approach prevents the catheter falling off due to biting and restlessness by the rats [23]. After the abdominal incision was closed, rats were placed in a restraining cage and allowed to recover from anesthesia for 2–3 h until they were awake. Saline (room temperature) was infused into the bladder at a constant low rate of 5 mL/h to induce a micturition reflex [24] and rats were kept under a heating lamp to prevent a reduction in body temperature during the experiment. Principal detection indices included: inter contraction interval (ICI), maximum cystometric capacity (MCC), maximal detrusor pressure (Pmax = Pves-Pabd), bladder compliance (BC), and non-voiding contractions (NVC). When finish, the rats were humanely euthanized using CO_2 inhalation. Their bladders were removed, trimmed, emptied of their contents, and then placed into individual, pre-weighed tubes to assess bladder weights.

2.7. Western blot analysis

When the protein was prepared, equal amounts of each protein sample was separated using 10% SDS polyacrylamide gels (PAGE) and transferred to polyvinylidene fluoride (PVDF) membranes. After blocking with 5% normal BSA, PVDF membranes were incubated with the following primary antibodies: rabbit anti-human-TRPC6 (1:500), rabbit anti-rat-TRPC6 (1:500), mouse anti-rat-FKBP12 (1:500) and mouse polyclonal primary anti-β-actin (1:3000) at 4 ˚C overnight. After washing, membranes were incubated specific horseradish peroxidase-conjugated anti-IgG secondary antibodies, and detected using an enhanced chemiluminescence (ECL) system [25,26]. The grayscale value of protein bands were analyzed using Image-J software (National Institutes of Health, Bethesda, MA, USA) and normalized to that of β-actin. Representative results of four independent experiments are shown.

2.8. Rreverse transcription-polymerase chain reaction (RT-PCR) and real-time quantitative PCR (qPCR) analysis

Total RNA was extracted from bladder smooth muscle tissues using Trizol. The RNA purity and quantitative analysis was performed, and the sample volumes were adjusted based on RNA concentrations to ensure equal total RNA amounts. Then the RNA was reverse transcribed into cDNA using oligo (dT) primers and an Omniscript RT Kit. RT-PCR was performed as pervious reported [27,28], with some modifications. The primers used for RT-PCR were designed and synthesized by TaKaRa (Shiga, Japan) as follows: human TRPC6 primers (NM_004621.5): sense, 5'-ACGCTTCGCTACCACCAG-3'; antisense, 5'-GGGACGACGGTG AAGCA-3', the amplicon was 196 bp; human β-actin primers (NM_001101.3): sense, 5'- TGGCACCCAGCACAATGAA-3'; antisense, 5'-CTAAGTCATAGTCCGCCTAGAAGCA-3', the amplicon was 186 bp; rat TRPC6 primers (NM_053559.1): sense, 5'-TGGCAAGTCCAGCATACCT GTC-3'; antisense, 5'-GTGTTTCTGCAGAGGTCCAGGAG-3', the amplicon was 178 bp; rat β-actin primers(NM_031144.2): sense, 5'-GGA GATTACTGCCCTGGCTCCTA-3'; antisense, 5'-GACTCATCGTACTCCTG CTTGCTG-3', the amlicon was 150 bp. PCR conditions were as follows: 94 ˚C for 2 min; and 30–35 cycles of 94 ˚C for 30 s, 56 ˚C for 30 s, and 72 ˚C for 40 s; and a final elongation of 7 min at 72 ˚C in a thermal cycler (Bio-Rad, USA).

qPCR was performed using SYBR®Premix Ex Taq™ II (TaKaRa) on a Mx3000 P instrument (Agilent Stratagene). The primers for qPCR were designed and synthesized by TaKaRa (Shiga, Japan) as follows: rat TRPC6 primer (NM_053559.1): sense, 5'-GGCTAATCGAGGACCAGCAT-3'; antisense, 5'-TTCTAGCATCTTCCGCACCA-3', the product length was 121 bp; rat β-actin primer (NM_031144.2): sense, 5'-TGTCACCAACTG GGACGATA-3'; antisense, 5'-GGGGTGTTGAAGGTCTCAAA-3', the product length was 165 bp. The gene expression relative to β-actin was calculated using Stratagene Mx3000 P software.

2.9. Immunofluorescence (IF) staining

The steps of IF for tissues and cells were basically similar as [29–31], with some modifications. Briefly, after incubation in the primary antibodies at 4 ˚C overnight and corresponding secondary antibodies at 37 ˚C for 1 h, the sections were stained with DAPI to visualize nucleus and images were captured using a laser confocal microscope of A1 (Nikon, Japan). The integrated optical densities (IOD) of all images were measured using Image-J software. Representative results of four independent experiments were shown.

2.10. Cell growth

Cell growth was determined by haemocytometer cell counting method [32]. Briefly, 5×10^4 cells per well were seeded into 6-well plates and cultured for 6, 12, 24, 36, 48, 72 and 96 h with or without PDGF (50 μg) and FK506 (10 μM). Cells were harvested by 0.25% trypsinisation, stained with trypan blue and counted with a haemocytometer to determine the number of cells.

2.11. Cell cycle analysis

Cell cycle analysis was performed as previously reported [33], with some modifications. Briefly, cells were treated with or without PDGF (50 μg) and FK506 (10 μM) for 24 h, and stored in ice cold ethanol (70%) at −20℃ overnight. The cells were washed twice and re-suspended in freshly prepared PI staining solution containing 0.2 μg PI, 0.2 μg DNase-free RNase A, and 0.25% (v/v) triton X-100 in PBS. After, incubation at 37℃ for 15 min, cells were then placed on ice in the dark. Stained cells were analysed using a C6 (BD Biosciences) flow cytometer, acquiring at least 10,000 single cell events per sample. Quantification of the percentage of cells in G0/G1, S, and G2/M phases of the cell cycle was performed using the Modfit LT (Verity Software House, USA).

2.12. Transient transfection of BSMCs with siRNAs

Transfection of BSMCs with Cy3-siRNAs against TRPC6 was performed as previously reported [34], with some modifications. TRPC6-targeted were designed and synthesized by RiboBio Biotechnology (Guangzhou, China). The target sequence for rat TRPC6 siRNAs (siRNA-TRPC6) was as follows: 5'-GCTCAGAAGATTTCCATTT-3', and the target sequence for negative control (siRNA-Con) was as follows: 5'-TTCTCC GAACGTGTCACGT-3'. BSMCs with 50–60% confluence were transfected with 80 nM siRNAs using Opti-MEM and Lipofectamine™ 3000 Reagent according to the manufacturer's protocols. After transfection for 48 h, BSMCs were used for the following experiments.

2.13. Time-lapse Ca^{2+} imaging experiments

Measurement of intracellular Ca^{2+} was performed as previously described [35,36], with some modifications. BSMCs, which were plated on 35 mm glass bottom cell culture dishes and in DMEM/F-12 medium (supplemented with 1% FBS) with or without PDGF (50 μg), SAR7334 (1 μM) and FK506 (10 μM) for 24 h, then incubated with 5 μM Fluo-4/

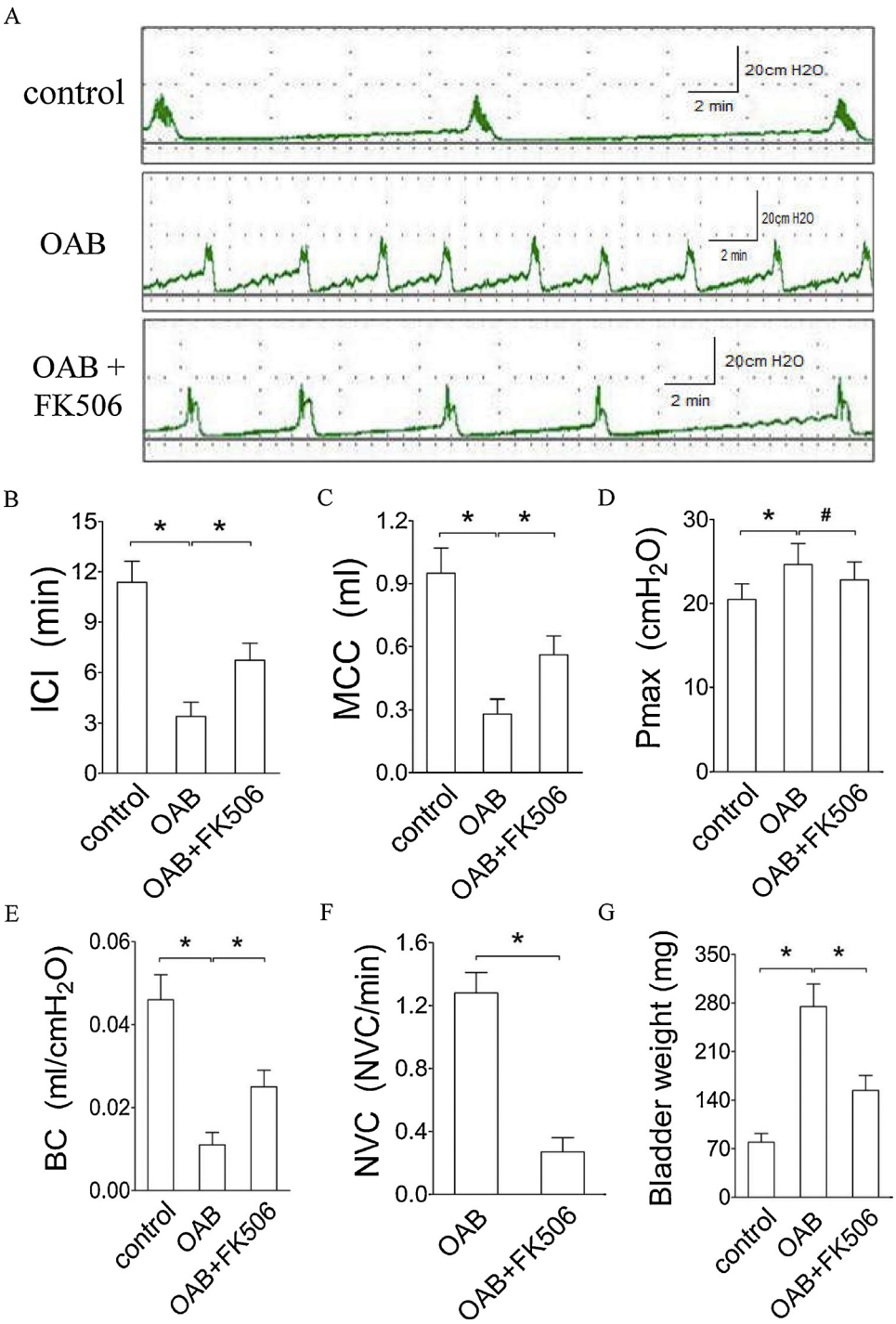

Fig. 1. Urodynamic recordings in the OAB rat model with or without FK506 treatment. (A) The urodynamic recordings of detrusor pressure obtained from control rats (with glucose, i.p; upper panel), OAB rats (with glucose, i.p.; middle panel) and OAB + FK506 rats (with 0.1 mg/kg/day FK506 and glucose, i.p.; lower panel) were recorded. (B–G) Analysis of cystometric parameters and bladder weight. Values are presented as means ± SD, n = 4, * $p < 0.01$ for comparison between control and OAB rats (ANOVA followed by Dunnett's post-hoc analysis), and # $p < 0.05$ and * $p < 0.01$ for respectively comparison between OAB and OAB + FK506 rats (ANOVA followed by Dunnett's post-hoc analysis, and except Student's *t*-test for NVC).

AM and 0.01% F-127 for 30 min at 37 °C in Hanks solution (containing 0.14 g $CaCl_2$). Cells were then washed with Hanks solution for 15 min at 37 °C to remove the extracellular excess of dye, and dye was deesterified for a minimum of 30 min at 37 °C with D-Hanks solution (containing 0 g $CaCl_2$). Ca^{2+} measurements were carried out using a laser confocal microscope of TCS-SP8 (Leica, Wetzlar, Germany) at room temperature. Fluo-4/AM was excited at 488 nm and recorded at 516 nm, and exposure time was 100 ms. Full images were collected every 5 s. Fluorescence intensity, which was used to represent changes in intracellular Ca^{2+} levels (fluorescence intensity after 0 mM $CaCl_2$, 0 mM $CaCl_2$ + 0.2 μM TG and 2 mM $CaCl_2$ in order of time precedence), were recorded. Data are expressed as normalized changes in background-corrected fluorescence emission (F/F0). All measurements are shown at the averages, which were measured for 20–30 cells, from of four independent experiments.

2.14. Collagen gel contraction experiments

About 80% confluent BSMCs were recovered from a culture dish using trypsin, washed with and suspended in DMEM/F-12 medium (with 1% FBS). Type-I collagen solution (5 μg), DMEM (10 times concentrated) and the cell suspension, which were prepared according to the manufacturer's instructions, were mixed carefully on ice at a ratio of 7:2:1. The final collagen suspension (1 μg), which was containing the BSMCs in 1×10^5 cells/mL without pre-treatment, at a volume of 300 μL was placed in each well of 24-well plates and gelated in an

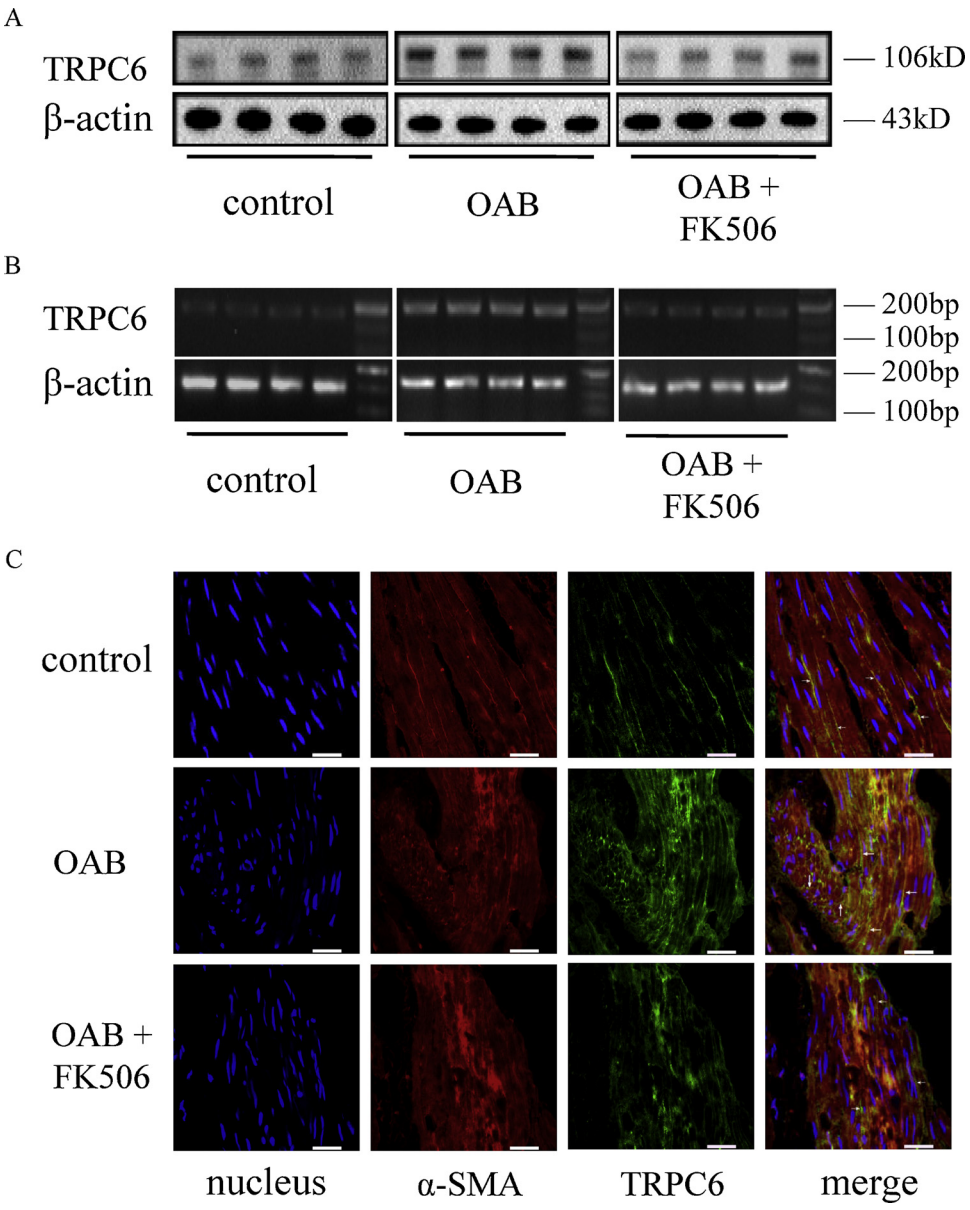

Fig. 2. Expression and distribution of TRPC6 in the OAB rat model with or without FK506 treatment. After testing urodynamic indices, the total bladder protein (A) and mRNA (B) was subjected to western blot and RT-PCR, respectively to measure TRPC6 amounts. β-actin was used to normalize expression amounts in both cases. (C) IF staining showing the localization of TRPC6 in rat bladder tissues. TRPC6 is stained green, nucleus is stained blue and α-SMA is stained red. White arrows indicates the TRPC6 on cell membrane in the merged images. Bar: 25 μm; magnification: 800 × (For interpretation of the references to colour in this figure legend, the reader is referred to the web version of this article).

incubator at 37 °C for 30 min. After gelation, 500 μL of DMEM/F-12 medium (with 10% FBS) was added onto the gel in each well and the cells in gel were further cultured at 37 °C in a 5% CO_2 atmosphere for 12 h. Then medium in each well was removed by aspiration and the gel was detached from well-wall using a new white (10 μL) pipette tip carefully, followed by 500 μL DMEM/F-12 medium (with 1% FBS) with or without PDGF (50 μg), SAR7334 (1 μM) and FK506 (10 μM) were added to each well, and collagen gel contraction was observed after 24 h. The surface area of the collagen gels was measured using Image-J software, and all experiments were performed in triplicate. The contraction (%) of gel surface area was expressed by the formula: [(area of 0 h - area of 24 h)/ area of 0 h] x100%. Representative results of four independent experiments are shown.

2.15. Co-immunoprecipitations (Co-IP)

Co-IP was performed as previous reported [10], with some modifications. Briefly, total lysates were prepared from BSMCs, and immunocomplexes were captured by incubating with protein A/G-agarose beads at 4 °C overnight. Beads were pelleted, washed four times with lysis buffer. Then, cell lysates and immunoprecipitated proteins were fractionated by SDS-PAGE, and the blots were probed with the indicated primary antibody and detected. To determine the effect of FK506 on FKBP12 interaction with TRPC6, total cell lysates, from PDGF (50 μg)-treated BSMCs were subjected to immunoprecipitation using anti-TRPC6 antibodies. Then the beads with attached immunocomplexes were washed and resuspended in lysate buffer containing different concentrations of FK506, and incubated for 30 min at 20 °C. The beads with immunocomplexes were subjected to centrifugation, and aliquots of beads and supernatants were probed using anti-FKBP12 antibody.

2.16. Statistical analysis

Values are expressed as mean ± SE, except for cystometric parameters and bladder weight, which are expressed as mean ± SD. Comparisons of two populations were made using Student's *t*-tests. For multiple comparisons with a single control, one-way analysis of variance (ANOVA) followed by Dunnett's post-hoc analysis was employed. Both analyses were performed using SigmaStat version 3.5.1 software (Jandel Scientific, San Rafael, CA). A statistically difference was defined as $p < 0.05$, and a statistically significant difference was defined as

$p < 0.01$.

3. Results

3.1. FK506 can improve urodynamic indices of BOO-induced OAB in rats

To explore the role of FK506 in OAB, we first established a rat OAB model using BOO. As shown in Fig. 1, urodynamic testing showed that rats with BOO experienced detrusor overactivity. A comparison of the main urodynamic indices between OAB rats and controls showed that ICI (control, 11.37 ± 1.26 min; OAB, 3.41 ± 0.85 min; n = 4), MCC (control, 0.95 ± 0.12 mL; OAB, 0.28 ± 0.07 mL; n = 4) and BC (control, 0.046 ± 0.006 mL/cmH_2O; OAB, 0.011 ± 0.003 mL/cmH_2O; n = 4) were all significantly lower in OAB rats than in controls. In contrast, Pmax (control, 20.47 ± 1.85 cmH_2O; OAB, 24.63 ± 2.51 cmH_2O; n = 4) and bladder weight (control, 79.42 ± 12.31 mg; OAB, 274.58 ± 32.61 mg; n = 4) were both significantly higher in OAB rats than in controls.

In parallel with FK506 administration, urodynamic indices in OAB rats showed improvements. Urodynamic tests showed that ICI (OAB, 3.41 ± 0.85 min; FK506, 6.72 ± 1.02 min; n = 4), MCC (OAB, 0.28 ± 0.07 mL; FK506, 0.56 ± 0.09 mL; n = 4) and BC (OAB, 0.011 ± 0.003 mL/cmH_2O; FK506, 0.025 ± 0.004 mL/cmH_2O; n = 4) were all significantly higher in FK506 rats than in OAB rats. In contrast, Pmax (OAB, 24.63 ± 2.51 cmH_2O; FK506, 22.81 ± 2.13 cmH_2O; n = 4), NVC (OAB, 1.28 ± 0.13 NVC/min; FK506, 0.27 ± 0.09 NVC/min; n = 4) and bladder weight (OAB, 274.58 ± 32.61 mg; FK506, 153.82 ± 21.64 mg; n = 4) were all significantly lower in FK506 rats as compared to OAB rats.

3.2. FK506 can inhibit TRPC6 expression in OAB rat bladder tissues

After testing urodynamic indices, we examined the expression and distribution of TRPC6 in control and OAB rats. As shown in Fig. 2, the amount of TRPC6 protein (control, 1.00 ± 0.18; OAB, 3.08 ± 0.22; n = 4; Fig. 2A and Fig. S1A) and mRNA (control, 1.00 ± 0.11; OAB, 2.78 ± 0.28; n = 4; Fig. 2B and Fig. S1B) were significantly elevated in OAB rats as compared to controls. Using IF, TRPC6 was largely located on membranes within bladder smooth muscle and distributed along muscular filaments. In samples from OAB rats, IF images revealed the increased staining intensity of TRPC6 (IOD; control, 817.16 ± 67.95; OAB, 2636.24 ± 398.94; n = 4; Fig. 2C and Fig. S1C). However, administration of FK506 inhibited the increases in both protein amount (OAB, 1.00 ± 0.11; FK506, 0.62 ± 0.08; n = 4) and mRNA expression (OAB, 1.00 ± 0.12; FK506, 0.37 ± 0.06; n = 4) of TRPC6 induced by OAB. Analysis of TRPC6 expression by IF confirmed that the increase in TRPC6 seen in OAB was reduced by FK506 treatment (IOD; OAB, 2636.24 ± 398.94; FK506, 1211.60 ± 110.45; n = 4). These data suggest that reducing the increased expression of TRPC6 seen in OAB maybe a potential means by which FK506 ameliorates the voiding dysfunction observed in OAB.

3.3. TRPC6 expression is increased in OAB clinical samples

Consistent with the results of OAB rats model, the expression of TRPC6 in OAB clinical samples was significantly elevated at both the protein amount (control, 1.00 ± 0.16; OAB, 2.79 ± 0.32; n = 4; Fig. 3A and Fig. S1D) and mRNA expression (control, 1.00 ± 0.08; OAB, 2.20 ± 0.16; n = 4; Fig. 3B and Fig. S1E) as compared to controls. IF staining confirmed TRPC6 expression in human bladder tissue and showed increased TRPC6 expression in OAB clinical samples (IOD, control, 744.25 ± 94.95; OAB, 2260.39 ± 328.34; n = 4; Fig. 3C and Fig. S1F). These data further confirmed that increased expression of TRPC6 might be a potential cause of OAB.

3.4. FK506 abolishes PDGF-induced TRPC6 upregulation and cellular proliferation in BSMCs

PDGF is one of the most important growth factors in bladder remodeling, thus we examined the possible involvement of PDGF in the induction of TRPC6 expression. As shown in Fig. S2, incubation of BSMCs with PDGF resulted in time/concentration-dependent increases in TRPC6 proteins, and PDGF (50 μg) for 24 h significantly increased the amount of TRPC6 protein. Knockdown of TRPC6 by siRNAs against TRPC6 significantly reduced PDGF-induced increase in both TRPC6 protein amount (Fig. 4A and S4A) and mRNA expression (Fig.4B and S4D) in BSMCs, further confirming that PDGF induced TRPC6 expression in BSMCs. These results provide a possible molecular mechanism for the elevation in TRPC6 expression observed in OAB.

As shown in Fig. 4C and S4B, PDGF-induced upregulation of TRPC6 was significantly abolished by FK506 in a dose-dependent manner (relative amount of TRPC6, basal, 1.00 ± 0.13; 50 μg PDGF, 2.91 ± 0.28; 50 μg PDGF + 10 μM FK506, 1.49 ± 0.13; n = 4). And qPCR tests also showed the similar results (relative TRPC6 mRNA expression, basal, 1.00 ± 0.09; 50 μg PDGF, 1.69 ± 0.09; 50 μg PDGF + 10 μM FK506, 1.12 ± 0.08; n = 4; Fig. 4D, S4E). In addition, IF results showed that the intensity of the immunostaining for TRPC6 in BSMCs was increased after PDGF treatment, and this effect was blocked by FK506 (IF IOD of TRPC6, basal, 637.53 ± 87.21; 50 μg PDGF, 1737.21 ± 102.52; 50 μg PDGF + 10 μM FK506, 987.26 ± 74.32; n = 4; Fig. 4E, S4C).

It has been reported that TRPC6 is a Ca^{2+}-peaceable ion channel, which regulates cell proliferation of smooth muscle cell [18]. As shown in Fig. 4F, cell numbers was significantly increased after PDGF (50 μg) treatment for more than 24 h, and FK506 (10 μM) significantly inhibited PDGF-induced increase in cell proliferation (cell numbers at 24 h for $x10^4$, control, 7.02 ± 1.69; control + 10 μM FK506, 7.26 ± 1.61; 50 μg PDGF, 14.16 ± 1.85; 50 μg PDGF + 10 μM FK506, 9.18 ± 1.76; n = 4). Flow cytometric analysis showed that PDGF (50 μg) treatment for 24 h resulted an increase of cells percentage in the S phase with a concomitant decrease in the G0/G1 phase (Fig. 4G, S4F), and this effect of PDGF was blocked by FK506 (10 μM).

3.5. FK506 abolishes TRPC6-mediated Ca^{2+} influx and contractility of BSMCs

In time-lapse Ca^{2+} imaging experiments, 0.2 μM TG was used to deplete endoplasmic Ca^{2+} stores, then 2 mM Ca^{2+} was added to the culture media (D-Hanks solution, containing 0 g $CaCl_2$) as an external Ca^{2+} source. As shown in Fig. 5A and S5A, PDGF treatment increased Ca^{2+} influx (Fluo-4, control, 1.00 ± 0.09; 50 μg PDGF, 1.93 ± 0.25; 50 μg PDGF + siRNA-Con, 1.88 ± 0.19; 50 μg PDGF + siRNA-TRPC6, 1.18 ± 0.15; n = 20–30; Fig.S5B) and decreased the time to the peak in BSMCs (Time, control, 400 ± 30 s; 50 μg PDGF, 345 ± 25 s; 50 μg PDGF + siRNA-Con, 350 ± 15 s; 50 μg PDGF + siRNA-TRPC6, 390 ± 20 s; n = 20–30; Fig.S5C). These effects were significantly inhibited by TRPC6 knockdown. Since PDGF treatment decreased the time to the peak in BSMCs after Ca^{2+} re-addition, and TRPC6 siRNAs blocked PDGF-induced early increase of cytosolic Ca^{2+}. TRPC6 channels may mediate PDGF-induced Ca^{2+} influx in BSMCs, and the early increase of cytosolic Ca^{2+} induced by PDGF may be caused by increased TRPC6 channel function after PDGF treatment.

Then, the TRPC6-specific inhibitor SAR7334 also significantly inhibited Ca^{2+} influx of BSMCs induced by PDGF (Fluo-4, control, 1.00 ± 0.11; 50 μg PDGF, 2.06 ± 0.22; 50 μg PDGF + 1 μM SAR7334, 1.23 ± 0.21; n = 20–30; Fig. 5B, S6A and B), and the time to the peak value was also shorter in the PDGF group as compared to the SAR73354 group (Time, control, 425 ± 25 s; 50 μg PDGF, 340 ± 15 s; 50 μg PDGF + 1 μM SAR7334, 385 ± 35 s; n = 20–30; Fig. S6C). Similar to the SAR7334, FK506 inhibited Ca^{2+} influx (2.06 ± 0.22 for 50 μg PDGF; 1.14 ± 0.23 for 50 μg PDGF + 10 μM FK506) with a prolonged

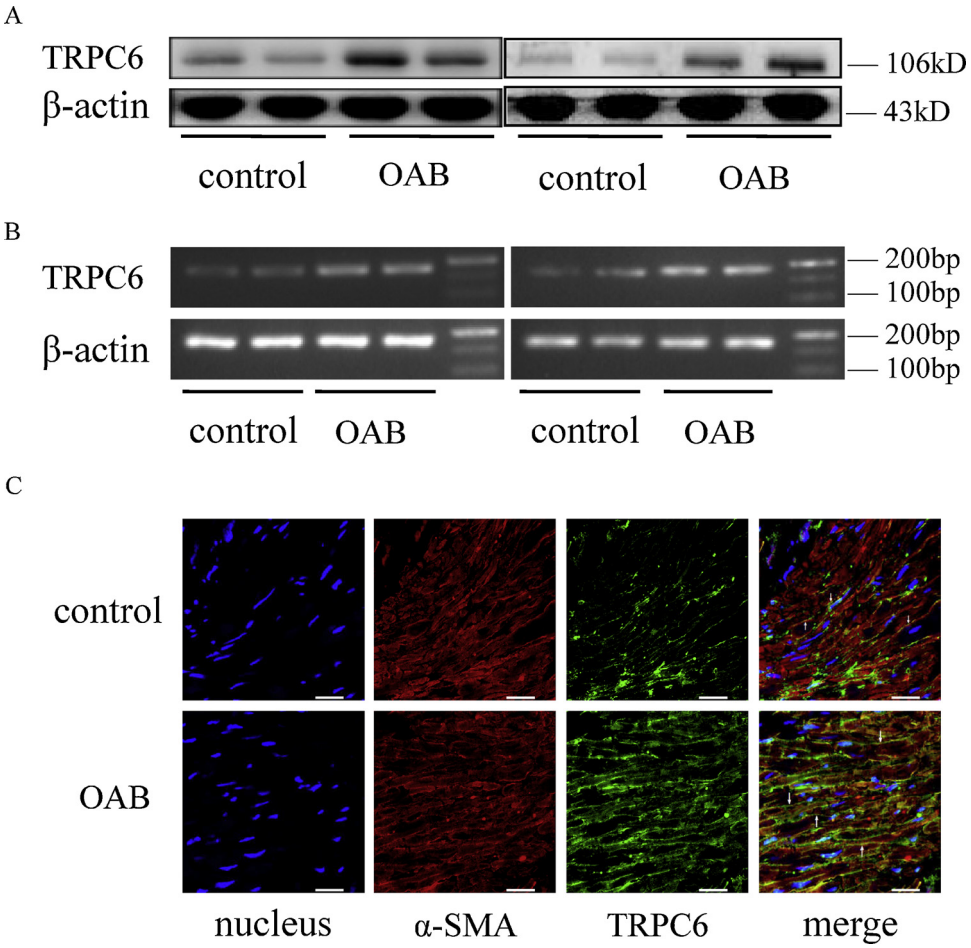

Fig. 3. Expression and distribution of TRPC6 in control and OAB human tissue samples. Protein amount (A) and mRNA expression (B) of TRPC6 in control and OAB tissues from humans were shown, respectively. β-actin was used as a loading control. (C) IF staining showing the localization of TRPC6 in bladder tissues. TRPC6 is stained green, nucleus is stained blue and α-SMA is stained red. White arrows indicates the TRPC6 on cell membrane in the merged images. Bar: 25 μm; magnification: 800 × (For interpretation of the references to colour in this figure legend, the reader is referred to the web version of this article).

time to the peak (340 ± 15 s for 50 μg PDGF; 395 ± 30 s for 50 μg PDGF + 10 μM FK506) and a delayed increase by approximately 40 s.

Similarly, PDGF (50 μg) enhanced contractility of BSMCs in collagen gel contraction experiments, and this effect was significantly inhibited by TRPC6 knockdown (basal, 40.63 ± 3.15%; 50 μg PDGF, 82.56 ± 5.37%; 50 μg PDGF + siRNA-Con, 79.62 ± 5.81%; 50 μg PDGF + siRNA-TRPC6, 46.37 ± 4.81%; n = 4; Fig. 5C, S5D), SAR7334 (1 μM) and FK506 (10 μM) (basal, 42.37 ± 3.82%; 50 μg PDGF, 85.23 ± 6.14%; 50 μg PDGF + 1 μM SAR7334, 51.73 ± 4.52%; 50 μg PDGF + 10 μM FK506, 53.25 ± 3.72%; n = 4; Fig. 5D, S6D).

3.6. FK506 inhibits PDGF-induced NFATc4 translocation to the nucleus and disrupts the interaction of TPRC6 with FKBP12

TRPC6 expression has been found to be directly regulated by calcineurin-NFAT signaling via acting on the TRPC6 promoter [37]. As shown in Fig. 6A, PDGF (50 μg) treatment increased the nuclear expression of NFATc4 and TRPC6 in BSMCs, and this effect was blocked by FK506 (10 μM). This result suggested that FK506 may inhibit PDGF-induced increase in TRPC6 expression by blocking NFATc4 translocation to the nucleus.

It has been reported that FK506 can interrupt the interaction of TRPC6 with FKBP12 [10]. Co-IP results showed that TRPC6 directly interacted with FKBP12 in BSMCs (Fig. 6B and C). To test the effect of FK506 on the interaction between TRPC6 and FKBP12, the immunocomplexes were incubated with increasing concentrations of FK506 (0–10 μM) after immunoprecipitation with anti-TRPC6. FKBP12 was completely associated with the agarose beads in the absence of FK506, and was partially or completely displaced from the beads and appeared in the supernatant in the presence of 0.5 and 10 μM FK506 (Fig. 6D). These results suggested that FK506 disrupted the interaction of TRPC6 with FKBP12 in BSMCs.

4. Discussion

Our results suggest that FK506 ameliorates urodynamic indices in OAB rats. Moreover, we herein demonstrate that TRPC6 is expressed in bladder smooth muscle, and that TRPC6 expression is elevated in OAB. FK506 administration suppresses the TRPC6 protein and mRNA elevation induced by BOO in rats, and improved urodynamic indices are associated with decreased TPRC6 in this study. We identified the potential involvement of PDGF-induced TRPC6 activation in the BSMCs, which was further supported by Ca^{2+} imaging and contractility results from BSMCs. Collectively, our data, which were obtained from urodynamic experiments and a combination of TRPC6 expression analyses performed in both OAB rats and humans, suggest that increased TRPC6 expression and activity may be partly responsible for some of the bladder dysfunction seen in OAB.

As an immunosuppressant drug, FK506 is widely used for renoprotective treatment in the clinic [7,8]. The results of this study confirm that FK506 ameliorates urodynamic indices in OAB rats,

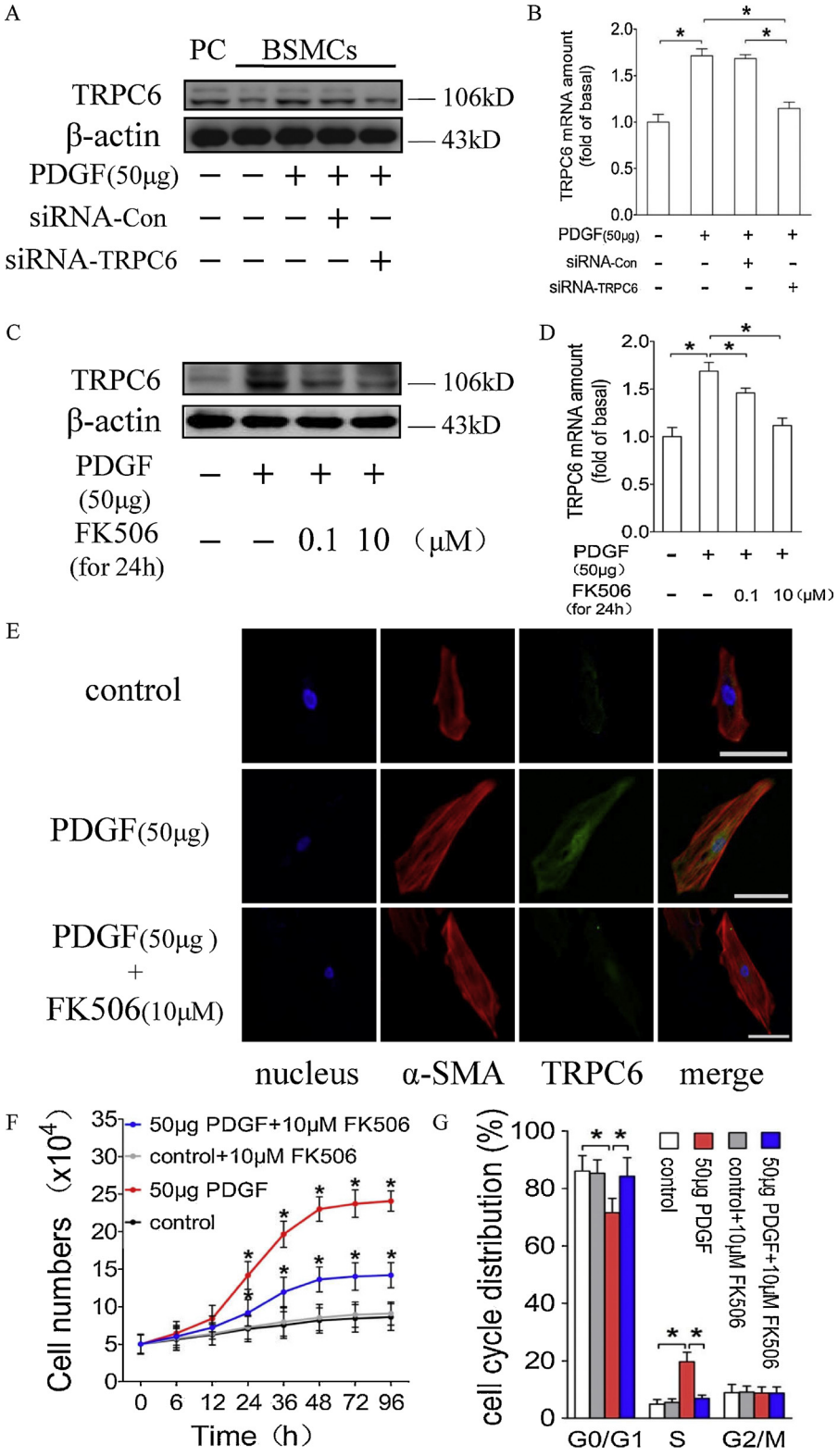

Fig. 4. FK506 inhibited PDGF-induced TRPC6 expression and cellular proliferation in BSMCs. The results of western blot and qPCR analysis shown that, TRPC6-siRNAs treatments for 48 h decreased both the TRPC6 protein amount (A) and mRNA expression (B) in BSMCs induced by PDGF. β-actin was used to normalize expression amounts in both cases. Normal rat kidney tissues were used as a positive control (PC). BSMCs were treated with 0.1 or 10 μM FK506 and 50 μg PDGF for 24 h, and total proteins (C) or mRNA (D) were subjected to western blot or qPCR analysis, respectively. β-actin was used to normalize expression amounts in both cases. (E) IF staining showing the localization of TRPC6 (green color) in BSMCs (nucleus is stained blue and α-SMA is stained red). Bar: 18 μm; magnification: 800 × . (F) Cell numbers in response to various stimuli at each indicated time point, and each data point represents the mean of four wells. Values are presented as means ± SE, n = 4, * $p < 0.01$ 50 μg PDGF vs. control, 50 μg PDGF + 10 μM FK506 vs. 50 μg PDGF (ANOVA followed by Dunnett's post-hoc analysis), (G) Flow cytometric analysis showing cell cycle distribution for each group at 24 h. Each data represents the mean of four wells. Values are presented as means ± SE, n = 4, * $p < 0.01$ 50 μg PDGF vs. control, 50 μg PDGF + 10 μM FK506 vs. 50 μg PDGF (ANOVA followed by Dunnett's post-hoc analysis) (For interpretation of the references to colour in this figure legend, the reader is referred to the web version of this article).

suggesting a potential therapeutic benefit of FK506 in OAB. And for older male patients requiring immunosuppressant treatment, FK506 administration may have the additional benefit of improving OAB symptoms, although FK506 can cause some adverse effect in men, such as hemorrhagic inflammation of the bladder. We also observed that downregulation of TRPC6 expression is the critical molecular event during FK506 treatment for OAB, and the molecular mechanisms involved in FK506-induced effects on TRPC6 still need to be delineated. It has been reported that FK506 can bind to the immunophilin FKBP12 to form an FK506-FKBP12 complex, and FK506 relaxed bladder smooth muscle by removing FKBP12 from the ryanodine receptor (RyR) Ca^{2+} release channel [38]. In addition, the FKBP12 is a binding partner of TRPC6, which recognizes specific XP dipeptides in partner proteins. Also it has been reported that, FK506 inhibited the TRPC6 channel, possibly through disrupting the interaction between FKBP12 and TRPC6 by mimicking the XP-binding motif [10]. In this study, we found

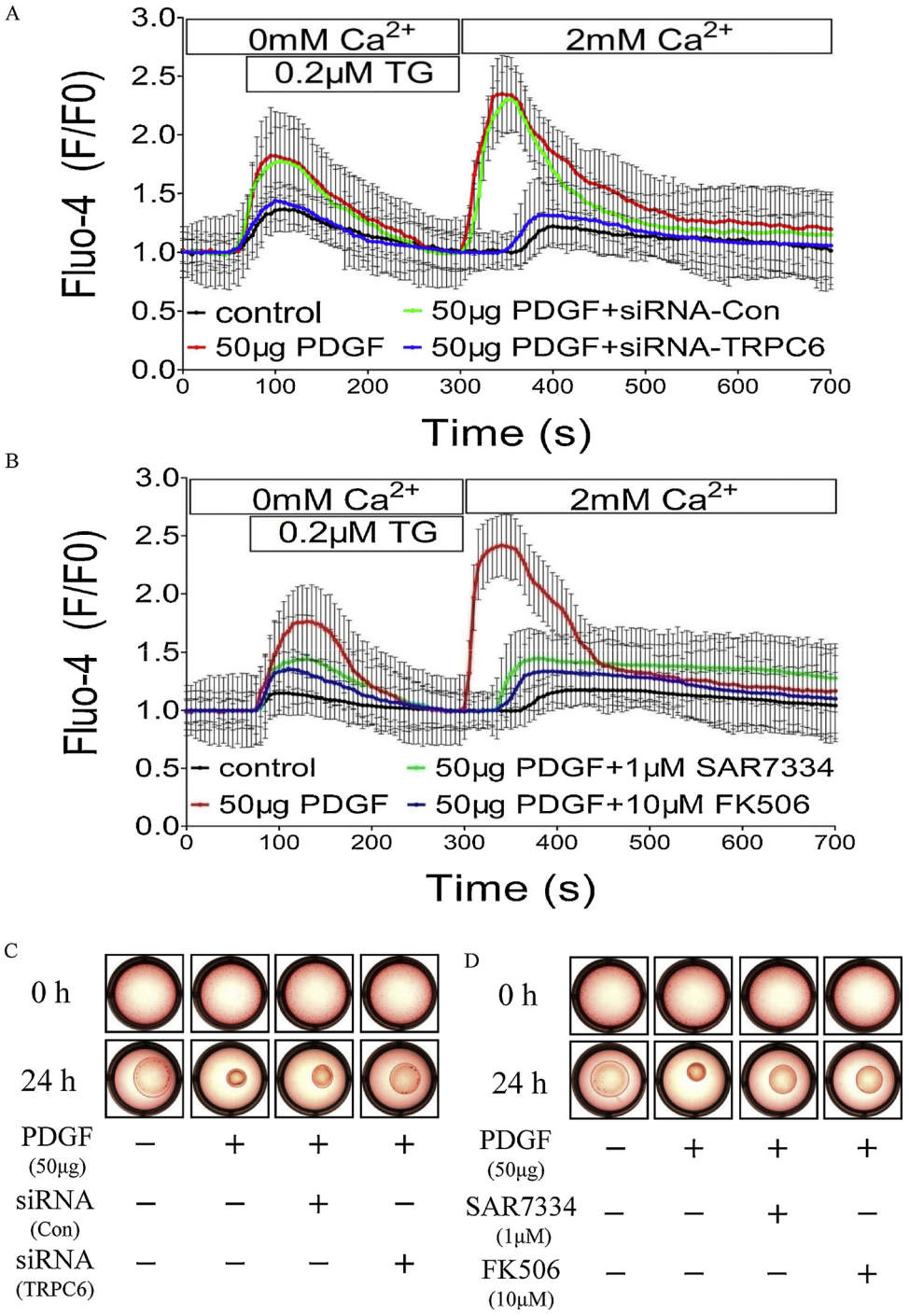

Fig. 5. FK506 abolished TRPC6-mediated Ca^{2+} influx and contractility of BSMCs. (A and B) The fluorescent intensity of Fluo-4 AM and time to peak value in control BSMCs, or BSMCs treated with PDGF, PDGF + siRNA-Con and PDGF + siRNA-TRPC6 (A), or BSMCs treated with PDGF, PDGF + SAR7334 and PDGF + FK506 (B). The first peak: release of Ca^{2+} evoked by 0.2 μM TG; the second peak: Ca^{2+} entry mediated by TRPC6. (C and D) Representative images of gel contraction in response to various stimuli.

that FK506 disrupted the interaction between TRPC6 and FKBP12 in BSMCs after PDGF treatment. Furthermore, TRPC6 transcription is dependent on NFAT-dependent activation by calcineurin, which plays an important role in bladder smooth muscle hypertrophy, and can be blocked by FK506 [39–43]. In the present study, we also found that FK506 reduced PDGF-induced TRPC6 expression by inhibiting NFATc4 translocation to the nucleus in BSMCs. Taken together, our findings suggest that FK506 inhibits PDGF-induced TRPC6 expression via inhibiting NFAT translocation to the nucleus, and reduces PDGF-induced TRPC6 function by disrupting its interaction with FKBP12 in BSMCs.

Increased spontaneous contractile activity of the detrusor is a well-known characteristic of OAB, and this is associated with higher intracellular Ca^{2+} levels within BSMCs [44,45]. The TRPC6 channel is a Ca^{2+}-permeable non-selective cation channel, and TRPC6 is reported to play a crucial role in the control of both Ca^{2+} entry and muscle contraction in smooth muscle cells. For example, it has reported that both TRPC6 and TRPC4 couple muscarinic receptors to depolarize in testinal smooth muscle cells, stimulate voltage-activated Ca^{2+}-influx, and cause contraction to accelerate small intestinal motility [9]. By RT-PCR experiments, it revealed that TRPC6 and TRPC4 were the only TRPC

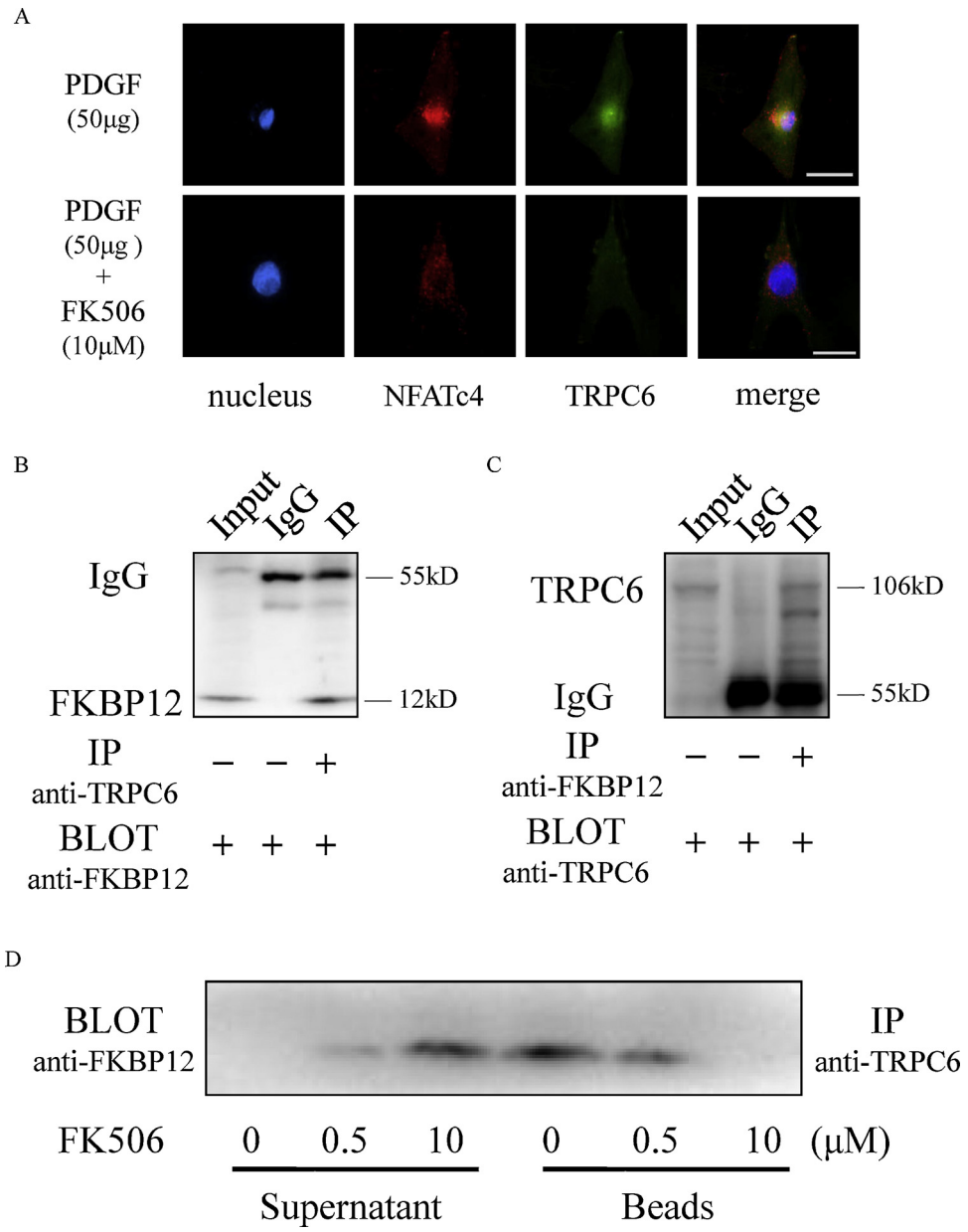

Fig. 6. FK506 reduced PDGF-induced NFAT translocation to the nucleus and disrupted the interaction of FKBP12 with TRPC6. (A) IF staining showing that 10 μM FK506 reduced TRPC6 (green color) expression by inhibiting NFATc4 (red color) translocation to the nucleus in BSMCs induced by 50 μg PDGF (nucleus is stained blue color). Bar: 18 μm; magnification: 800 × . (B and C) Co-IP showing the interaction between TRPC6 and FKBP12. The antibodies used for immunoprecipitation and immunoblotting are indicated below each lane. (D) The effect of FK506 on the interaction between TRPC6 and FKBP12. The beads with attached immunocomplexes were resuspended in lysate buffer containing FK506 at the concentration shown below each lane. FKBP12 was partially or completely displaced from the beads and appeared in the supernatant in the presence of 0.5 and 10 μM FK506 (For interpretation of the references to colour in this figure legend, the reader is referred to the web version of this article).

subtypes expressed in isolated murine detrusor myocytes, and that muscarinic receptor-mediated contraction of the detrusor involves the activation of TRPC4β channels [13,14]. Several studies have shown that knockdown of TRPC6 significantly increased the latency of Ca^{2+} spiking in A7r5 vascular smooth muscle cells and hippocampal neurons [46,47]. The data presented herein show that bladder muscle tissues obtained from OAB patients or OAB rat model have higher TRPC6 expression, and improved urodynamic indices are associated with attenuation of TRPC6 elevation in OAB rats. In in-vitro experiments, the enhanced activity and contractility in BSMCs induced by PDGF could be inhibited by SAR7334, the specific inhibitor of the TRPC6. Therefore, there is a close correlation between OAB and elevation of TRPC6 activity. Our results coincide with previous findings, and increase our understanding of the role of TPRC6 in the detrusor.

The role of PDGF in bladder remodeling is well-known. In the bladder, expression of PDGF and its receptors is increased under mechanical strain and contribute to increased bladder wall thickness in cases of BOO [16,17]. PDGF shares the same signaling pathway with that used by mechanical stimulation in inducing various BSMC responses [17,48,49]. A previous study reported that PDGF induced TRPC6 expression in pulmonary artery smooth muscle cells [18], and another study reported that PDGF direct and prompt induced the activation of TRPC6 channel in MEFs cells [50]. Furthermore, we also found that similar to PDGF, VEGF (100 μg) upregulated TRPC6 expression (Fig. S7A), promoted cellular proliferation (Fig. S7B), enhanced Ca^{2+} influx (Fig. S7C) and increased contractility (Fig. S7D) of BSMCs. These findings suggest that both PDGF and VEGF can contribute to TRPC6 upregulation in BSMCs.

Standard methods to create BOO in rats include distal urethral ligation and bladder neck-proximal urethral ligation [23]. Compared with distal ligation, proximal ligation must be made via an open-abdominal operation, which can cause infection, intestinal obstruction, stones and other complications; however, this model produces more powerful simulative for BPH. In the present study, we improved the methodology used to create a BOO rat model of OAB, using PVC tubes instead of silk sutures for bladder neck ligation. Compared with traditional silk suture, PVC tubes are elastic when compressing the bladder outlet, which effectively simulates the process of chronic progressive obstruction. Additionally, PVC tubes have a larger contact surface with the bladder neck to avoid tissue necrosis caused by tight suture ligation.

5. Conclusions

Our findings could have important clinical implications. We confirmed that FK506 improves urodynamic indices in OAB rats and that TRPC6 expression increases in bladder tissues of both OAB rats and humans. We further confirmed FK506 inhibits the increased expression of TRPC6 seen in OAB rat bladder tissues. These data suggest that TRPC6 elevation may contribute to OAB symptoms. Furthermore, our study has suggested that inhibiting the enhanced activity of TRPC6 seen in BSMCs could improve the function of detrusor. These results can potentially be important for patients with OAB, because FK506 may be used to improve clinical symptoms of OAB and TRPC6 may serve as an attractive target for therapeutic intervention for OAB.

Author contributions

Ping Wang, Baoman Li and Liu Cao conceived and designed the study; Cheng Chang, Sinan Jiang and Kai Li performed the experiments and analyzed the data; Cheng Chang and Kai Li wrote the paper; Ping Wang revised the whole paper. All authors have read and approved the final article.

Declarations of interest

All the authors have declared that no competing interest exists.

Acknowledgments

This work was supported by National Nature Science Foundation of China PR: (31271238) to Ping Wang, and (31200616) to Kai Li.

Appendix A. Supplementary data

Supplementary material related to this article can be found, in the online version, at doi:https://doi.org/10.1016/j.ceca.2018.11.007.

References

[1] A.J. Wein, E.S. Rovner, Definition and epidemiology of overactive bladder, Urology 60 (2002) 7–12 PubMed PMID: 12493342.
[2] S. Kajioka, N. Seki, N. Shahab, T. Yunoki, S. Naito, Etiology of overactive bladder and its therapeutic perspective—focusing on a myogenic basis for the overactive bladder, Fukuoka Igaku Zasshi 101 (2010) 94–100 PubMed PMID: 20845720.
[3] G. Kaneko, K. Nishimoto, Y. Ito, A. Uchida, The combination therapy of prednisolone and tacrolimus for severe painful bladder syndrome/interstitial cystitis, Can. Urol. Assoc. J. 6 (2012) E46–49 PubMed PMID: 22511431.
[4] C.N. Dave, F. Chaus, M.B. Chancellor, M. Lajness, K.M. Peters, Innovative use of intravesical tacrolimus for hemorrhagic radiation cystitis, Int. Urol. Nephrol. 47 (2015) 1679–1681 PubMed PMID: 26347076.
[5] Y.C. Chuang, P. Tyagi, H.Y. Huang, et al., Intravesical immune suppression by liposomal tacrolimus in cyclophosphamide-induced inflammatory cystitis, Neurourol. Urodyn. 30 (2011) 421–427 PubMed PMID: 20860016.
[6] B.R. Rajaganapathy, J.J. Janicki, P. Levanovich, et al., Intravesical liposomal tacrolimus protects against radiation cystitis induced by 3-beam targeted bladder radiation, J. Urol. 194 (2015) 578–584 PubMed PMID: 25839382.
[7] R. Ma, L. Liu, W. Jiang, Y. Yu, H. Song, FK506 ameliorates podocyte injury in type 2 diabetic nephropathy by down-regulating TRPC6 and NFAT expression, Int. J. Clin. Exp. Pathol. 8 (2015) 14063–14074 PubMed PMID: 26823720.
[8] Y. Shengyou, Y. Li, H. Zhihong, M. Yuanyuan, Influence of tacrolimus on podocyte injury inducted by angiotensin II, J. Renin. Syst. 16 (2015) 260–266 PubMed PMID: 25650384.
[9] Y. Kamiyama, S. Muto, H. Masuda, et al., Inhibitory effects of nicorandil, a K ATP channel opener and a nitric oxide donor, on overactive bladder in animal models, BJU Int. 101 (2008) 360–365 PubMed PMID: 18070173.
[10] W.G. Sinkins, M. Goel, M. Estacion, W.P. Schilling, Association of immunophilins with mammalian TRPC channels, J. Biol. Chem. 279 (2004) 34521–34529 PubMed PMID: 15199065.
[11] J.C. Gonzalez-Cobos, M. Trebak, TRPC channels in smooth muscle cells, Front. Biosci. Landmark Ed. (Landmark Ed.) 15 (2010) 1023–1039 PubMed PMID: 20515740.
[12] N. Onohara, M. Nishida, R. Inoue, et al., TRPC3 and TRPC6 are essential for angiotensin II-induced cardiac hypertrophy, EMBO J. 25 (2006) 5305–5316 PubMed PMID: 17082763.
[13] V.V. Tsvilovskyy, A.V. Zholos, T. Aberle, et al., Deletion of TRPC4 and TRPC6 in mice impairs smooth muscle contraction and intestinal motility in vivo, Gastroenterology 137 (2009) 1415–1424 PubMed PMID: 19549525.
[14] C.S. Griffin, E. Bradley, S. Dudem, et al., Muscarinic Receptor Induced Contractions of the Detrusor are Mediated by Activation of TRPC4 Channels, J. Urol. 196 (2016) 1796–1808 PubMed PMID: 27287524.
[15] T. Gevaert, J. Vriens, A. Segal, et al., Deletion of the transient receptor potential cation channel TRPV4 impairs murine bladder voiding, J. Clin. Invest. 117 (2007) 3453–3462 PubMed PMID:17948126.
[16] C. Akbal, S.D. Lee, C. Jung, R. Rink, M. Kaefer, Upregulation of both PDGF-BB and PDGF-BB receptor in human bladder fibroblasts in response to physiologic hydrostatic pressure, J. Pediatr. Urol. 2 (2006) 402–408 PubMed PMID: 18947646.
[17] L. Preis, A. Herlemann, R.M. Adam, H.G. Dietz, R. Kappler, M. Stehr, Platelet derived growth factor has a role in pressure induced bladder smooth muscle cell hyperplasia and acts in a Paracrine Way, J. Urol. 194 (2015) 1797–1805 PubMed PMID: 26055827.
[18] Y. Yu, M. Sweeney, S. Zhang, O. Platoshyn, J. Landsberg, A. Rothman, et al., PDGF stimulates pulmonary vascular smooth muscle cell proliferation by upregulating TRPC6 expression, Am. J. Physiol. Cell Physiol. 284 (2003) C316–330 PubMed PMID: 12529250.
[19] S. Chauvet, L. Jarvis, M. Chevallet, N. Shrestha, K. Groschner, A. Bouron, Pharmacological characterization of the native store-operated calcium channels of cortical neurons from embryonic mouse brain, Front. Pharmacol. 7 (2016) 486 PubMed PMID: 28018223.
[20] D.V. Ilatovskaya, O. Palygin, V. Levchenko, B.T. Endres, A. Staruschenko, The role of angiotensin II in glomerular volume dynamics and podocyte calcium handling, Sci. Rep. 7 (2017) 299 PubMed PMID: 28331185.
[21] T. Maier, M. Follmann, G. Hessler, et al., Discovery and pharmacological characterization of a novel potent inhibitor of diacylglycerol-sensitive TRPC cation channels, Br. J. Pharmacol. 172 (2015) 3650–3660 PubMed PMID: 25847402.
[22] R.C. Cavalli, R. Tambara Filho, P. Gomes Rde, D.A. Veronez, J. Slongo, R. Fraga, Analysis of the histology of the scar bladder and biochemical parameters of rats with a solitary kidney undergoing immunosuppression with tacrolimus, Acta Cir. Bras. 29 (2014) 508–514 PubMed PMID: 25140592.
[23] A. Malmgren, C. Sjogren, B. Uvelius, A. Mattiasson, K.E. Andersson, P.O. Andersson, Cystometrical evaluation of bladder instability in rats with infravesical outflow obstruction, J. Urol. 137 (1987) 1291–1294 PubMed PMID: 3586176.
[24] S. Du, I. Araki, M. Yoshiyama, T. Nomura, M. Takeda, Transient receptor potential channel A1 involved in sensory transduction of rat urinary bladder through C-fiber pathway, Urology 70 (2007) 826–831 PubMed PMID: 17991581.
[25] K. Li, J. Yao, L. Shi, N. Sawada, Y. Chi, Q. Yan, et al., Reciprocal regulation between proinflammatory cytokine-induced inducible NO synthase (iNOS) and connexin43 in bladder smooth muscle cells, J. Biol. Chem. 286 (2011) 41552–41562 PubMed PMID: 21965676.
[26] K. Li, J. Yao, N. Sawada, M. Kitamura, K.E. Andersson, M. Takeda, Beta-Catenin signaling contributes to platelet derived growth factor elicited bladder smooth muscle cell contraction through up-regulation of Cx43 expression, J. Urol. 188 (2012) 307–315 PubMed PMID: 22608743.
[27] C. Vandebrouck, D. Martin, M. Colson-Van Schoor, H. Debaix, P. Gailly, Involvement of TRPC in the abnormal calcium influx observed in dystrophic (mdx) mouse skeletal muscle fibers, J. Cell Biol. 158 (2002) 1089–1096 PubMed PMID: 12235126.
[28] Y. Wang, D. Yue, K. Li, Y.L. Liu, C.S. Ren, P. Wang, The role of TRPC6 in HGF-induced cell proliferation of human prostate cancer DU145 and PC3 cells, Asian J. Androl. 12 (2010) 841–852 PubMed PMID: 20835261.
[29] Z. Li, K. Li, J. Wang, X. Zhai, L. Wang, N. Ohno, et al., MRT letter: application of novel "in vivo cryotechnique" in living animal kidneys, Microsc. Res. Tech. 76 (2013) 113–120 PubMed PMID: 23132785.
[30] K. Li, J. Wang, X. Yin, X. Zhai, Z. Li, Alteration of podocyte protein expression and localization in the early stage of various hemodynamic conditions, Int. J. Mol. Sci. 14 (2013) 5998–6011 PubMed PMID: 23502465.
[31] Y. Zhao, K. Takeyama, S. Sawatsubashi, et al., Corepressive action of CBP on androgen receptor transactivation in pericentric heterochromatin in a Drosophila experimental model system, Mol. Cell. Biol. 29 (2009) 1017–1034 PubMed PMID: 19075001.
[32] P.A. Nguyen, T.A.V. Pham, Effects of platelet-rich plasma on human gingival fibroblast proliferation and migration in vitro, J. Appl. Oral Sci. 26 (2018) e20180077PubMed PMID: 29995149.
[33] E. Smith, H.M. Palethorpe, Y. Tomita, et al., The purified extract from the medicinal plant bacopa monnieri, bacopaside II, inhibits growth of colon cancer cells in vitro by inducing cell cycle arrest and apoptosis, Cells 7 (2018) pii: E81. PubMed PMID: 30037060.
[34] Shaojun Li, Yilin Pan, Rui Ke, et al., Inhibition of phosphodiesterase-5 suppresses calcineurin/NFAT-mediated TRPC6 expression in pulmonary artery smooth muscle cells, Sci. Rep. 7 (2017) 6088 PubMed PMID: 28729555.
[35] A.M. Fontainhas, A.G. Obukhov, M.C. Nowycky, Protein kinase Calpha modulates depolarizaton-evoked changes of intracellular Ca2+ concentration in a rat pheochromocytoma cell line, Neuroscience 133 (2005) 393–403 PubMed PMID: 15878642.
[36] K. Iwatsubo, S. Suzuki, C. Li, et al., Dopamine induces apoptosis in young, but not in neonatal, neurons via Ca2+-dependent signal, Am. J. Physiol., Cell Physiol. 293 (2007) C1498–1508 PubMed PMID: 17804610.
[37] K. Kuwahara, Y. Wang, J. McAnally, J.A. Richardson, R. Bassel-Duby, J.A. Hill, et al., TRPC6 fulfills a calcineurin signaling circuit during pathologic cardiac remodeling, J. Clin. Invest. 116 (2006) 3114–3126 PubMed PMID: 17099778.
[38] T. Weidelt, G. Isenberg, Augmentation of SR Ca(2+) release by rapamycin and FK506 causes K(+)-channel activation and membrane hyperpolarization in bladder

smooth muscle, Br. J. Pharmacol. 129 (2000) 1293–1300 PMID:10742283.
[39] P.R. Langford, L. Keyes, M.D. Hansen, Plasma membrane ion fluxes and NFAT-dependent gene transcription contribute to c-met-induced epithelial scattering, J. Cell. Sci. 125 (2012) 4001–4013 PubMed PMID: 22685327.
[40] F.J. Dumont, FK506, an immunosuppressant targeting calcineurin function, Curr. Med. Chem. 7 (2007) 731–748 PubMed PMID: 10702636.
[41] A. Dietrich, T. Gudermann, TRPC6: physiological function and pathophysiological relevance, Handb. Exp. Pharmacol. 222 (2014) 157–188 PubMed PMID: 24756706.
[42] A. Dietrich, T. Gudermann, Trpc6, Handb. Exp. Pharmacol. 179 (2007) 125–141 PubMed PMID: 17217054.
[43] K.1 Nozaki, K. Tomizawa, T. Yokoyama, et al., Calcineurin mediates bladder smooth muscle hypertrophy after bladder outlet obstruction, J. Urol. 170 (2003) 2077–2081 PMID:14532857.
[44] G.V. Petkov, Role of potassium ion channels in detrusor smooth muscle function and dysfunction, Nat. Rev. Urol. 9 (2011) 30–40 PubMed PMID: 22158596.
[45] S. Chacko, E. Cortes, M.J. Drake, C.H. Fry, Does altered myogenic activity contribute to OAB symptoms from detrusor overactivity? ICI-RS 2013, Neurourol. Urodyn. 33 (2014) 577–580 PubMed PMID: 24838314.
[46] Bharath K. Mani, Lioubov I. Brueggemann, Leanne L. Cribbs, et al., Opposite regulation of KCNQ5 and TRPC6 channels contributes to vasopressin-stimulated calcium spiking responses in A7r5 vascular smooth muscle cells, Cell Calcium 45 (2009) 400–411 PubMed PMID: 19246091.
[47] Hua Zhang, Suya Sun, Lili Wu, et al., Store-operated calcium channel complex in postsynaptic spines: a new therapeutic target for alzheimer's disease treatment, J. Neurosci. 36 (2016) 11837–11850 PubMed PMID: 27881772.
[48] M. Stehr, R.M. Adam, J. Khoury, et al., Platelet derived growth factor-BB is a potent mitogen for rat ureteral and human bladder smooth muscle cells: dependence on lipid rafts for cell signaling, J. Urol. 169 (2003) 1165–1170 PubMed PMID: 12576874.
[49] R.M. Adam, J.A. Roth, H.L. Cheng, et al., Signaling through PI3K/Akt mediates stretch and PDGF-BB-dependent DNA synthesis in bladder smooth muscle cells, J. Urol. 169 (2003) 2388–2393 PubMed PMID: 12771803.
[50] L. Lei, S. Lu, Y. Wang, et al., The role of mechanical tension on lipid raft dependent PDGF-induced TRPC6 activation, Biomaterials 35 (2014) 2868–2877 PubMed PMID: 24397990.